Electrochemical Properties of Nano-sized $Li_4Ti_5O_{12}$ Powders Prepared by Flame Spray Pyrolysis

Jung Hyun Kim, Yun Chan Kang[*]

Department of Chemical Engineering, Konkuk University, 1 Hwayang-dong, Gwangjin-gu, Seoul 143-701, Korea
[*]E-mail: yckang@konkuk.ac.kr

Nanosized $Li_4Ti_5O_{12}$ powders are prepared from a spray solution with a 15 % excess of lithium using a flame spray pyrolysis process. The mean particle size of the precursor powders is 23 nm. The $Li_4Ti_5O_{12}$ powders obtained after post-treatment at 700°C have small amounts of rutile TiO_2 impurities and have a mean particle size of 47 nm. Post-treatment at 800°C, however, produces phase-pure $Li_4Ti_5O_{12}$ powders with a mean particle size of 300 nm. The initial discharge capacities of the $Li_4Ti_5O_{12}$ powders are 132, 160, and 151 mAh g^{-1} for post-treatment temperatures of 600, 700, and 800°C, respectively, and the Coulombic efficiencies are 87 %, 92 %, and 99 %. The hard aggregation between the particles and growth of the particles to submicron sizes that occur at a high post-treatment temperature of 800°C make a large proportion of the $Li_4Ti_5O_{12}$ grains inactive, lowering the specific capacity. The discharge capacities of the powders post-treated at 700°C decrease from 160 to 157 mAh g^{-1} over 50 cycles, and the capacity retention is 98 %.

1. INTRODUCTION

Spinel lithium titanate ($Li_4Ti_5O_{12}$) has good Li^+ insertion and de-insertion reversibility, exhibits zero strain volume change during charge and discharge cycles, and achieves excellent safety performance, which makes it an attractive anode material for Li-ion batteries [1-9]. Furthermore, nanosized powders provide short diffusion lengths and more active surface areas for Li^+ intercalation [10-13]. For these reasons, there has been extensive study on the characteristics of nanosized $Li_4Ti_5O_{12}$ powders prepared using various solid-state and liquid-solution methods [14-20]. However, the preparation of nanosized $Li_4Ti_5O_{12}$ powders via gas-phase reaction methods has been much less well studied [21,22]. One such gas-phase reaction method, flame spray pyrolysis, has been shown to have

certain advantages for the preparation of aggregation-free nanosized powders with complex compositions [23-27] and has been used to synthesize various anode and cathode materials for Li-ion batteries [22,28-32]. In particular, nanosized $Li_4Ti_5O_{12}$ powders have been prepared via flame spray pyrolysis using nonaqueous solvents such as xylene [21]. Metal alkoxides of Li and Ti components were dissolved into the non-aqueous solution. The directly obtained $Li_4Ti_5O_{12}$ powders had particle sizes of several tens of nanometers, and the main impurity was rutile TiO_2 that remained because of the short residence time of the powders inside the high-temperature flame. Post-treatment of these powders to obtain $Li_4Ti_5O_{12}$ powders with fewer impurities resulted in rapid particle growth and hard particle aggregation [22].

In this study, nanosized $Li_4Ti_5O_{12}$ powders were prepared from an aqueous spray solution of lithium nitrate and titanium(IV) tetraisopropoxide using high-temperature flame spray pyrolysis. The physical and electrochemical properties of the nanosized $Li_4Ti_5O_{12}$ powders formed from the spray solution with excess lithium were compared to those of powders formed from a spray solution with a stoichiometric amount of lithium.

2. EXPERIMENTAL

Nanosized $Li_4Ti_5O_{12}$ powders were synthesized from titanium(IV) tetraisopropoxide (TTIP, $Ti[OCH(CH_3)_2]_4$) and lithium nitrate ($LiNO_3$) using a high-temperature flame spray pyrolysis setup consisting of a droplet generator, a flame nozzle, a quartz reactor, a powder collector, and a blower [33]. Propane (fuel) and oxygen (oxidizer) were used to produce the diffusion flame. The flow rate of the fuel gas was 5 L min^{-1}, and the flow rates of the oxidizer and carrier gases were fixed at 40 L min^{-1} and 10 L min^{-1}, respectively. A 1.7 MHz ultrasonic spray generator with six resonators was used to generate the droplets, which were then carried into the high-temperature diffusion flame by the oxygen carrier gas. A mixed solvent with a volume ratio of ethyl alcohol to distilled water of 3:7 was used to produce a spray solution with an overall concentration of the lithium and titanium components of 0.5 M. The excess amounts of lithium dissolved in the spray solution were 0 % and 15 % of the stoichiometric amount. To improve the crystallinity and remove possible impurity phases, the as-prepared powders obtained by the flame spray pyrolysis procedure were post-treated in a box furnace at temperatures between 600 and 800°C for 3 h in an air atmosphere. The crystal structures of the post-treated powders were investigated by performing X-ray diffractometry (XRD, Rigaku DMAX-33) analyses using Cu Kα radiation at room temperature. The morphological characteristics of the powders were investigated using field-emission transmission electron microscopy (FETEM, JEOL, JEM-2100F). The electrode was fabricated using a mixture of 20 mg of $Li_4Ti_5O_{12}$, 2.5 mg of carbon black (Super P), and 2.5 mg of polytetrafluoroethylene (PTFE). Lithium metal and a microporous polypropylene film were used as the counter electrode and separator, respectively. The electrolyte (Techno Semichem Co.) was 1 M $LiPF_6$ in a 1:1 mixture by volume of ethylene carbonate/dimethyl carbonate (EC/DMC). The entire cell was assembled in a glove box in an argon atmosphere. The charge/discharge characteristics of the samples were determined by performing potential cycling in the range 1−3 V at a current density of 0.1 C.

3. RESULTS AND DISCUSSION
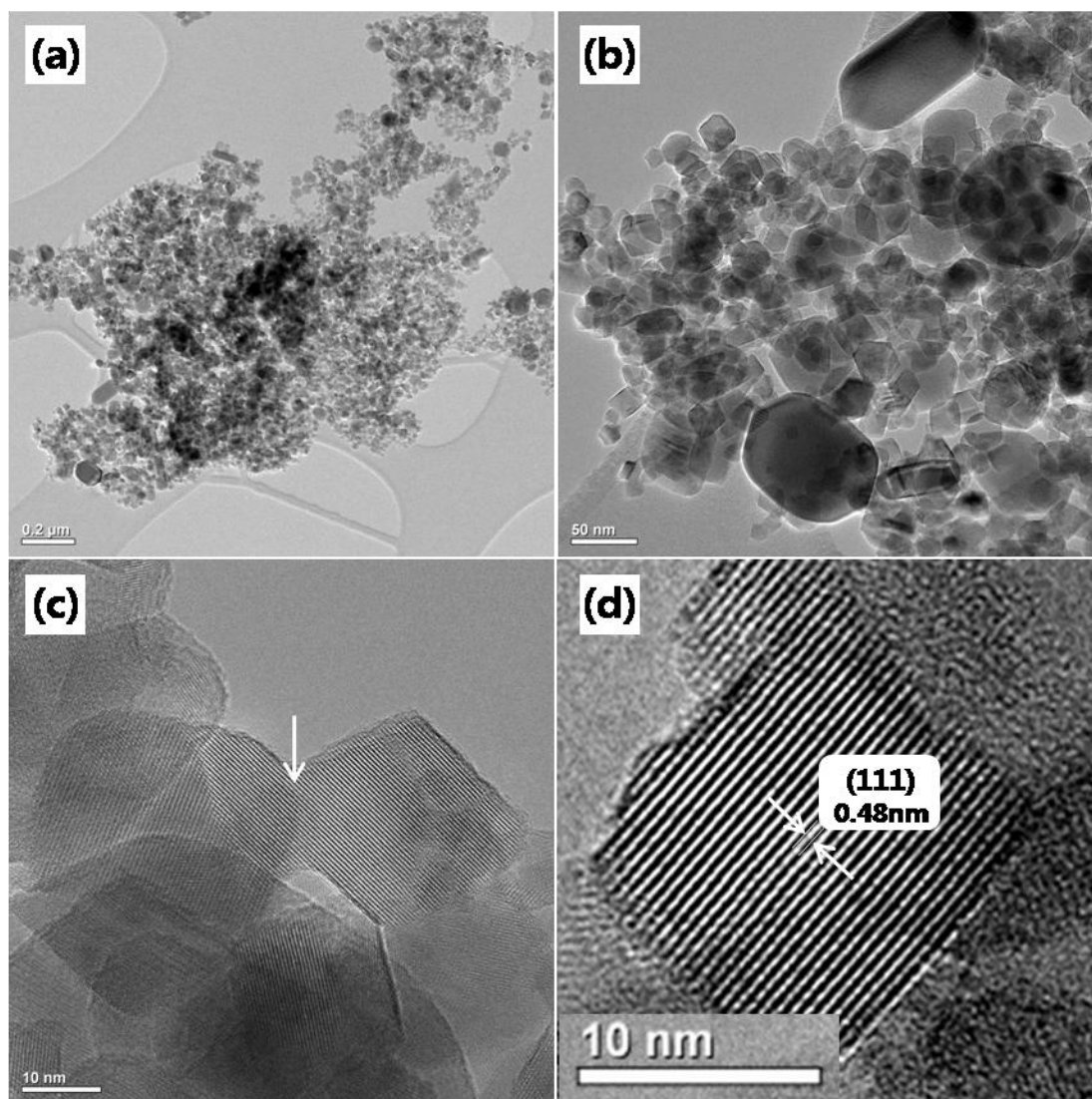
Figure 1. TEM images of the $Li_4Ti_5O_{12}$ powders directly prepared by flame spray pyrolysis.

During the flame spray pyrolysis, micron-sized mixed oxide powders were first formed as an intermediate product after drying and decomposition of droplets containing of Li and Ti components. Then, complete evaporation of the Li_2O and TiO_2 occurred inside the high-temperature diffusion flame, irrespective of whether there was an excess of lithium. Therefore, the $Li_4Ti_5O_{12}$ nanopowders were formed by nucleation and growth processes from the evaporated vapors. Fig. 1 shows TEM images of the $Li_4Ti_5O_{12}$ powders prepared from the spray solution with a 15 % excess of Li using flame spray pyrolysis. All the powders prepared via flame spray pyrolysis consisted of nanosized particles. The mean particle size of the precursor powders measured from the TEM images was 23 nm. Necking between the nanopowders was observed in the TEM image, as shown by the arrow in Fig. 1(c). This necking between particles resulted from the high number concentration of the nanopowders inside the high-temperature diffusion flame due to the high concentration of the spray solution, 0.5 M, which resulted in many collisions. The high-resolution TEM image of the powders shows a single-

crystalline structure and had a clear lattice fringe spacing of approximately 0.48 nm, which corresponds to the (111) interplanar spacing in $Li_4Ti_5O_{12}$. Thus, highly crystalline $Li_4Ti_5O_{12}$ powders were directly prepared by high-temperature flame spray pyrolysis.
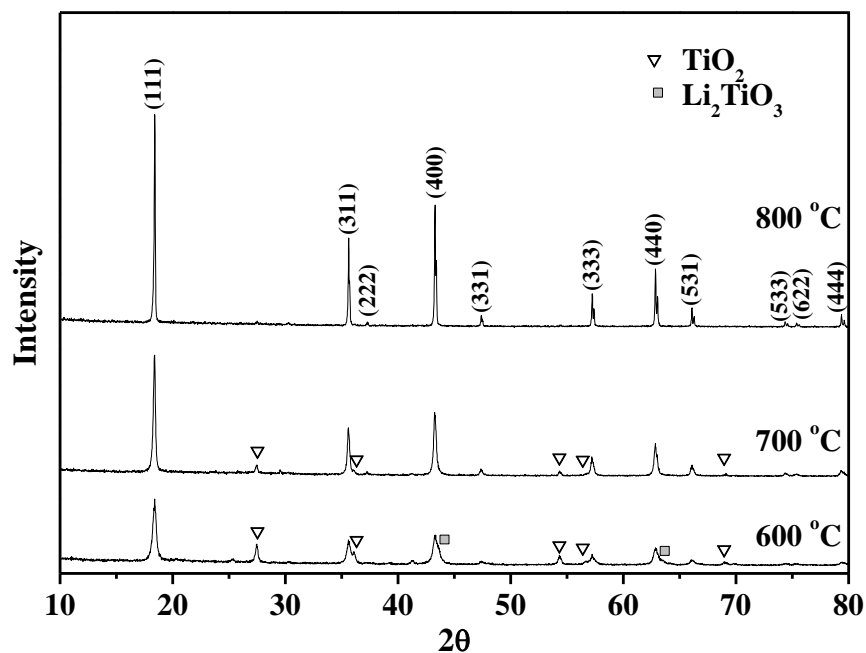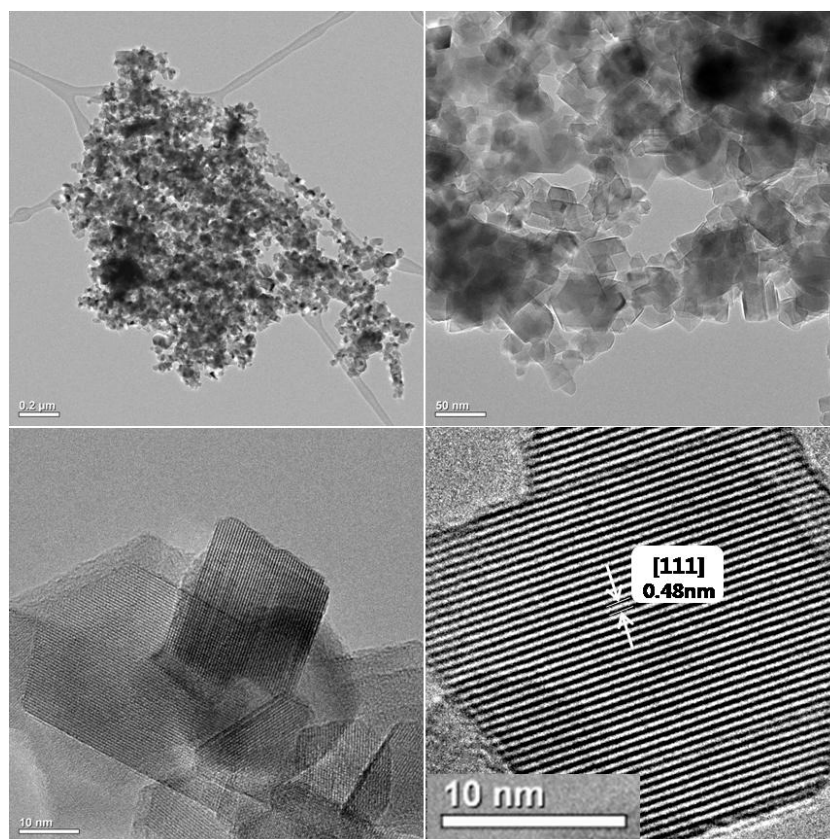

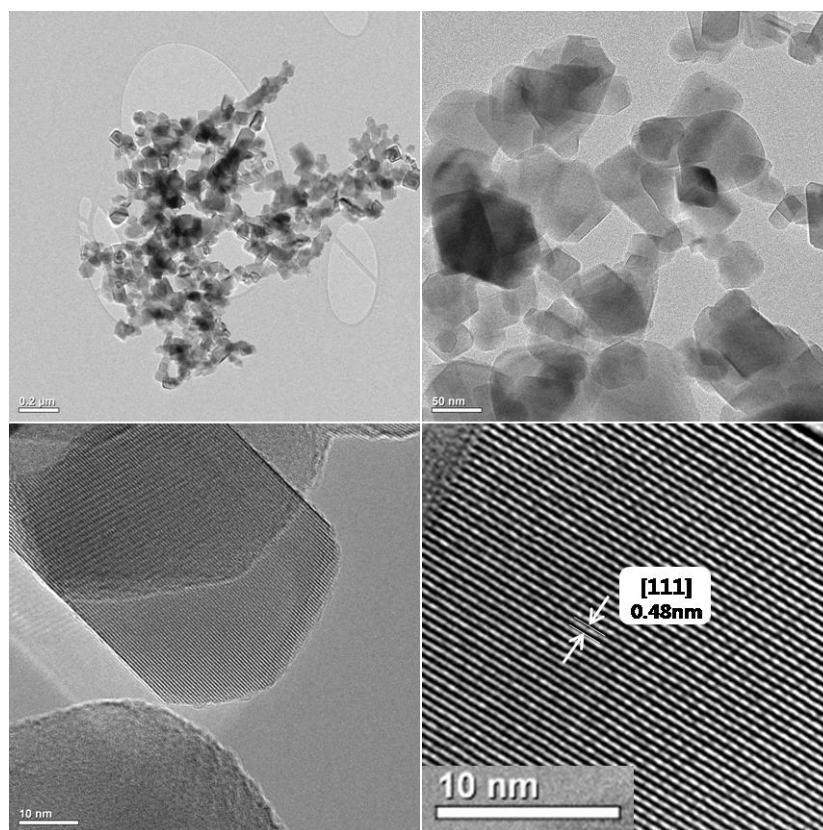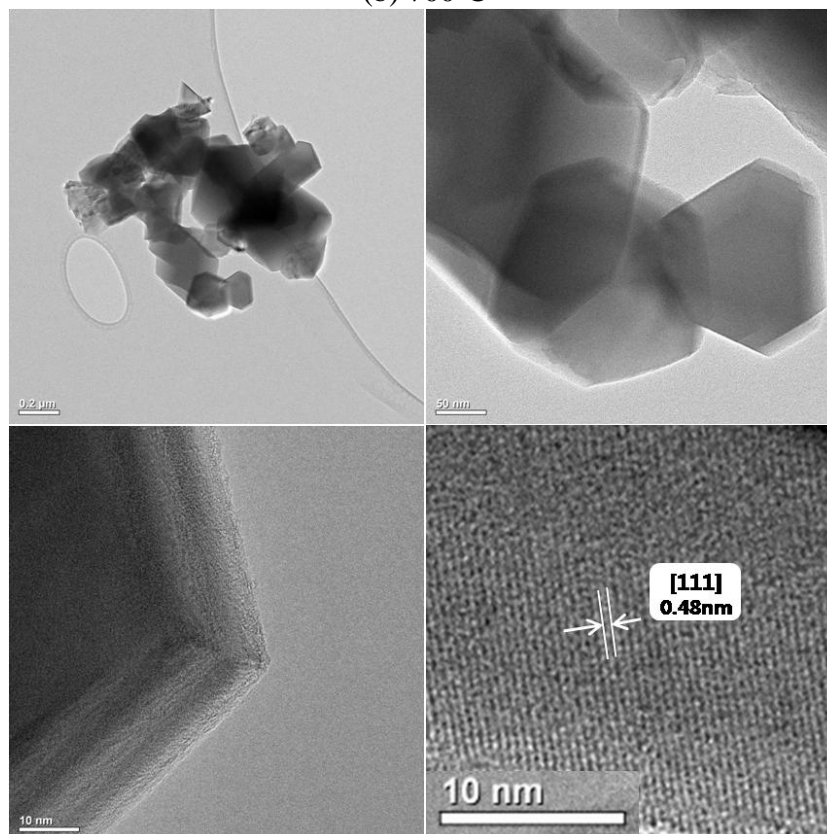**Figure 2.** XRD patterns of the $Li_4Ti_5O_{12}$ powders post-treated at different temperatures with 15 % excess amount of lithium.
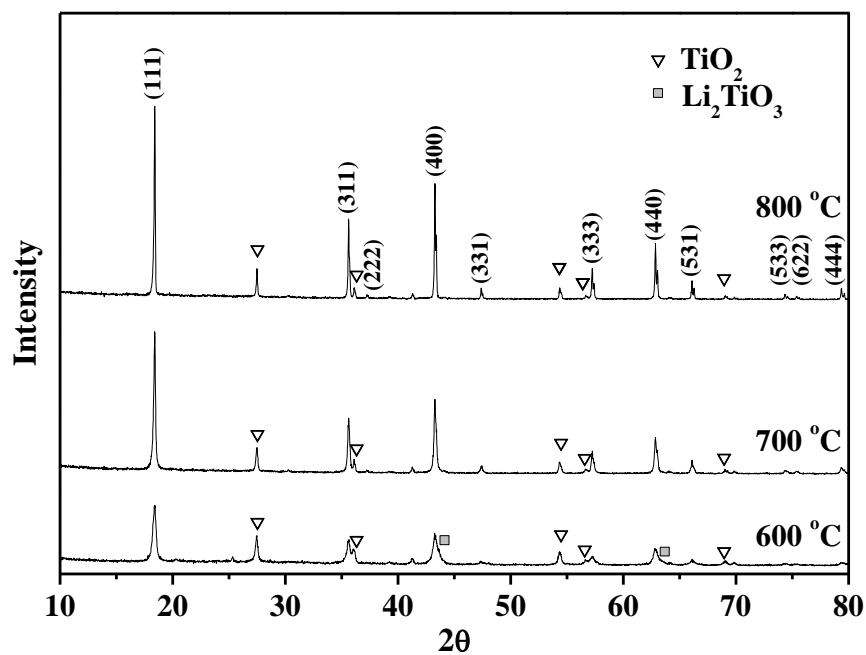
Figure 3. XRD patterns of the $Li_4Ti_5O_{12}$ powders post-treated at different temperatures without an excess amount of lithium.

Figs. 2 and 3 show the XRD patterns of the post-treated $Li_4Ti_5O_{12}$ powders prepared from the spray solutions with and without an excess of lithium. The XRD patterns (not shown here) of the powders directly prepared by flame spray pyrolysis showed that the main crystal structures were spinel $Li_4Ti_5O_{12}$ (JCPDS Card No. 26-1198) and rutile TiO_2 phases with small peaks corresponding to Li_2TiO_3 (JCPDS Card No. 33-0831), irrespective of the presence of excess lithium. Phase-pure $Li_4Ti_5O_{12}$ powders were not directly obtained after flame spray pyrolysis because of the extremely short residence time of the powders inside the high-temperature diffusion flame. The small peak corresponding to the Li-inactive Li_2TiO_3 phase was observed when the post-treatment temperature was low, i.e., 600°C. Jiang et al. showed that for powders produced using a sol-gel process, the Li_2TiO_3 phase would also coexist with the main $Li_4Ti_5O_{12}$ phase when the sintering temperature was 600°C [34]. Fig. 2 shows that with increasing post-treatment temperature, the diffraction peaks of the spinel $Li_4Ti_5O_{12}$ phase become sharper, and the peak intensities for rutile TiO_2 decrease. Eventually, phase-pure spinel $Li_4Ti_5O_{12}$ powders were formed at a post-treatment temperature of 800°C. Fig. 2 also shows that the XRD pattern of the $Li_4Ti_5O_{12}$ powders post-treated at 700°C had small peaks corresponding to rutile TiO_2. However, the TiO_2 phase remained in the powders formed from the spray solution without an excess of lithium, as shown in the XRD pattern of the powders post-treated at a high temperature of 800°C in Fig. 3. Thus, lithium-deficient precursor powders were prepared from the spray solution without an excess of lithium. The mean crystallite sizes for the rutile TiO_2 phase of the powders prepared from the spray solution without an excess of lithium increased from 33 to 82 nm when the post-treatment temperature was increased from 600 to 800°C.

(a) 600°C
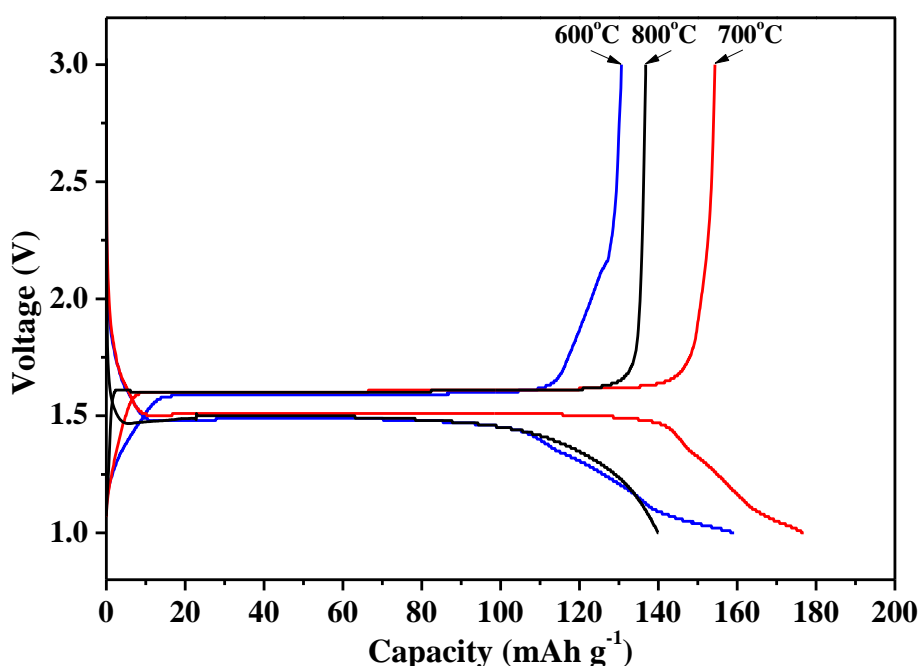
(b) 700°C

(c) 800°C

Figure 4. TEM images of the $Li_4Ti_5O_{12}$ powders post-treated at different temperatures with 15 % excess amount of lithium.

Fig. 4 shows the TEM images of the post-treated $Li_4Ti_5O_{12}$ powders prepared from the spray solution with a 15 % excess amount of lithium. The high-resolution TEM image of the post-treated powders again showed a single-crystalline structure and had a clear lattice fringe spacing of approximately 0.48 nm corresponding to the (111) interplanar spacing in $Li_4Ti_5O_{12}$. The powder post-treated at 600°C had a similar mean particle size and morphology to those of the precursor powders directly prepared by flame spray pyrolysis. The $Li_4Ti_5O_{12}$ powders post-treated at 700°C, which had small impurity peaks corresponding to rutile TiO_2, had a mean particle size of 47 nm and slight particle aggregation. However, abrupt particle growth and hard aggregation between the particles occurred at a high post-treatment temperature of 800°C. The mean particle size of the powders post-treated at 800°C was 300 nm.

Figure 5. Initial charge/discharge curves of the $Li_4Ti_5O_{12}$ powders post-treated at different temperatures without an excess amount of lithium.

Figs. 5 and 6 show the initial charge-discharge curves of the post-treated $Li_4Ti_5O_{12}$ powders prepared from the spray solutions without and with excess lithium. The slopes were observed before and after the voltage plateaus for the charge and discharge processes for the powders post-treated at temperatures of 600 and 700°C in Figs. 5 and 6. The areas of the slope of the voltage curves may indicate single-phase regions. The nanometer sizes of the $Li_4Ti_5O_{12}$ powders post-treated at low temperatures resulted in these distinct single-phase regions. Extension of the single-phase region was already reported for high-surface-area $Li_4Ti_5O_{12}$ [22,35]. The initial discharge capacities of the powders prepared from the spray solution without excess lithium were 131, 154, and 137 mAh g^{-1} for post-treatment temperatures of 600, 700, and 800°C, respectively, as shown in Fig. 5, and the Coulombic efficiencies were 82, 87, and 98 %. As shown in Fig. 2, the mean crystallite size for the

rutile TiO_2 phase of the powders increased from 33 to 82 nm when the post-treatment temperature was increased from 600 to 800°C. However, the peak intensities of the rutile TiO_2 phase did not change for different post-treatment temperatures.
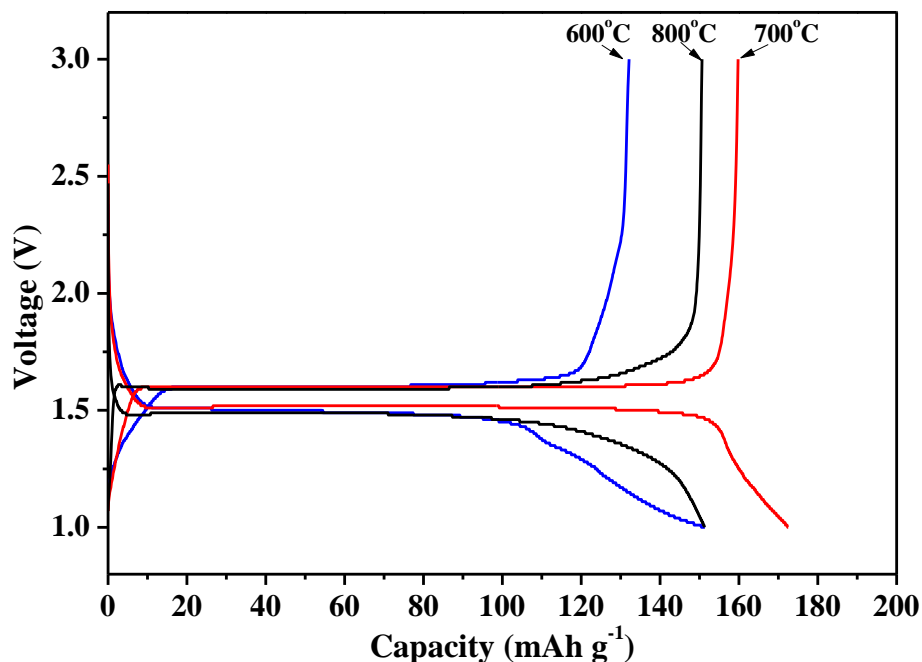
**Figure 6.** Initial charge/discharge curves of the $Li_4Ti_5O_{12}$ powders post-treated at different temperatures with 15 % excess amount of lithium.

Nanometer-sized rutile TiO_2 exhibited a much higher electroactivity towards lithium insertion than micrometer-sized rutile TiO_2 [36,37]. Furthermore, electrochemical cycling experiments on nanosized rutile showed a high degree of insertion and de-insertion irreversibility [36,38]. Therefore, this irreversibility of the $Li_4Ti_5O_{12}$ powders formed from a spray solution without excess lithium decreased as the post-treatment temperature increased because of the crystal growth of the rutile TiO_2 and the particle growth from nanometer to submicron sizes. The initial discharge capacities of the $Li_4Ti_5O_{12}$ powders prepared from the spray solution with a 15% excess of lithium were 132, 160, and 151 mAh g^{-1} for post-treatment temperatures of 600, 700, and 800°C, respectively, as shown in Fig. 6, and the Coulombic efficiencies were 87, 92, and 99 %. The increase in post-treatment temperature from 600 to 800°C decreased the irreversible capacity loss in the first cycles for the $Li_4Ti_5O_{12}$ powders prepared from the spray solution with excess lithium for two reasons: (1) the decrease in the amount of the rutile TiO_2 phase with its high irreversible capacity loss and (2) the particle growth from sizes of several tens nanometers to submicron sizes [36,38]. The powders post-treated at 700°C had the highest initial discharge capacity, irrespective of the lithium content of the spray solution. The phase-pure $Li_4Ti_5O_{12}$ powder post-treated at 800°C also had a lower initial discharge capacity than that of the powders with TiO_2 impurities, as shown in Fig. 6. Previous study of $Li_4Ti_5O_{12}$ has indicated that the hard aggregation between nanoparticles can decrease the powder's discharge capacity [39]. It is

believed that such hard aggregation between the particles and the growth of the particles to submicron sizes at the high post-treatment temperature of 800°C make a large proportion of the $Li_4Ti_5O_{12}$ grains inactive, lowering the specific capacity.
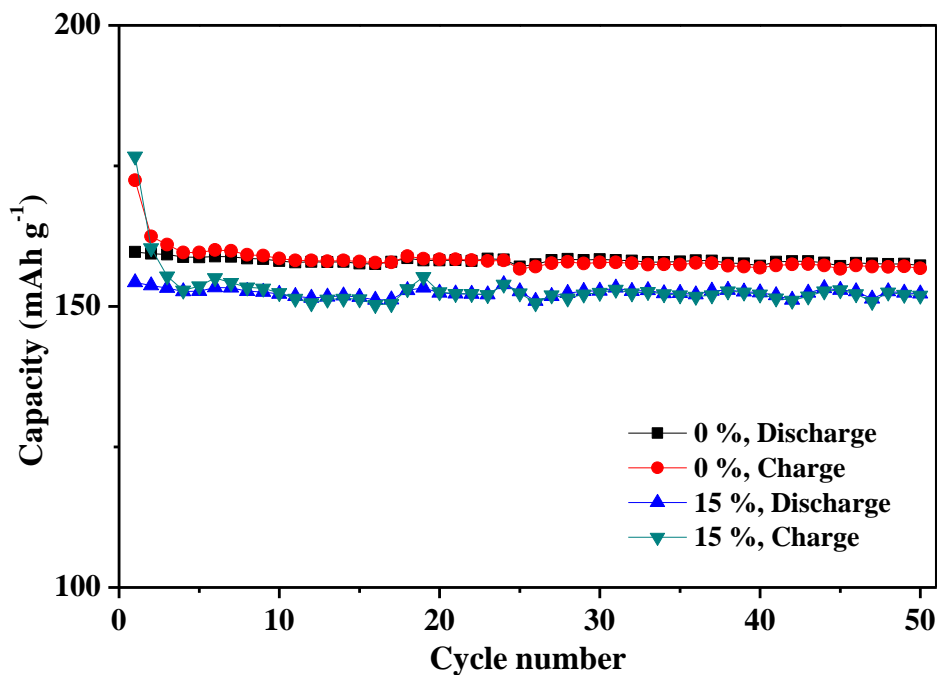
Figure 7. Cycling performances of the $Li_4Ti_5O_{12}$ powders post-treated at a temperature of 700°C.

Fig. 7 shows the cycle performance of $Li_4Ti_5O_{12}$ powders prepared from the spray solutions without and with excess lithium. The $Li_4Ti_5O_{12}$ powders post-treated at 700°C were cycled at a constant current density of 0.1 C. The discharge capacities of the powders prepared from the spray solution without excess lithium decreased from 154 to 151 mAh g^{-1} over 50 cycles, while the discharge capacities of the powders prepared from the spray solution with a 15 % excess of lithium decreased from 160 to 157 mAh g^{-1} over 50 cycles. Thus, the capacity retention was 98 % irrespective of the presence of excess lithium. The Coulombic efficiencies of the powders increased during the first several cycles and then became saturated above 99 %, irrespective of the lithium content of the spray solution. The powder formed from the spray solution with a 15 % excess amount of lithium had a higher discharge capacity than the powder formed from the spray solution without excess lithium because of its phase homogeneity and its low amount of the rutile TiO_2 phase.

4. CONCLUSIONS

$Li_4Ti_5O_{12}$ powders were prepared from the spray solutions with and without excess lithium using flame spray pyrolysis. The optimum amount of excess lithium in order to obtain $Li_4Ti_5O_{12}$ powders with the best electrochemical properties was 15 %. The $Li_4Ti_5O_{12}$ powders had particle sizes

of several tens nanometers and slight particle aggregation even after post-treatment at a high temperature of 700°C. The increase in post-treatment temperature from 600 to 800°C decreased the irreversible capacity loss in the first cycles for the $Li_4Ti_5O_{12}$ powders prepared from the spray solution with excess lithium for two reasons: (1) the decrease in the amount of the rutile TiO_2 phase with its high irreversible capacity loss and (2) the particle growth from sizes of several tens nanometers to submicron sizes. The $Li_4Ti_5O_{12}$ nanopowders with small amounts of rutile TiO_2 impurities had higher discharge capacities than did the phase-pure $Li_4Ti_5O_{12}$ powders with submicron particle sizes.

References

1. T. Ohzuku, A. Ueda, N. Yamamoto, *J. Electrochem. Soc.*, 142 (1995) 1431.
2. E. Ferg, R.J. Gummow, A. de Kock, M.M. Thackeray, *J. Electrochem. Soc.*, 141 (1994) L147.
3. K.M. Colbow, J.R. Dahn, R.R. Haering, *J. Power Sources*, 26 (1989) 397.
4. K. Zaghib, M. Simoneau, M. Armand, M. Gauthier, *J. Power Sources*, 81-82 (1999) 300.
5. S. Takai, M. Kamata, S. Fujine, K. Yoneda, K. Kanda, T. Esaka, *Solid State Ionics*, 123 (1999) 165.
6. A.S. Arico, P. Bruce, B. Scrosati, J-M. Tarascon, W. van Schalkwijk, *Nat. Mater.*, 4 (2005) 366.
7. B. Li, F. Ning, Y.B. He, H. Du, Q.H. Yang, J. Ma, F. Kang, C.T. Hsu, *Int. J. Electrochem. Sci.*, 6 (2011) 3210.
8. C.H. Chen, J.T. Vaughey, A.N. Jansen, D.W. Dees, A.J. Kahaian, T. Goacher, M.M. Thackeray, *J. Electrochem. Soc.*, 148 (2001) A102.
9. S.H. Ju, Y.C. Kang, *J. Power Sources*, 195 (2010) 4327.
10. C. Jiang, M. Wei, Z. Qi, T. Kudo, I. Honma, H. Zhou, *J. Power Sources*, 166 (2007) 239.
11. P. Poizot, S. Laruelle, S. Grugeon, L. Dupont, J.M. Tarascon, *Nature*, 407 (2000) 496.
12. J. Xu, C. Jia, B. Cao, W.F. Zhang, *Electrochim. Acta*, 52 (2007) 8044.
13. Y. Xia, P. Yang, Y. Sun, Y. Wu, B. Mayers, B. Gates, Y. Yin, F. Kim, H. Yan, *Adv. Mater.*, 15 (2003) 353.
14. H. Ge, N. Li, D. Li, C. Dai, D. Wang, *Electrochem. Commun.*, 10 (2008) 1031.
15. H. Ge, N. Li, D. Li, C. Dai, D. Wang, *Electrochem. Commun.*, 10 (2008) 719.
16. C.Y. Ouyang, Z.Y. Zhong, M.S. Lei, *Electrochem. Commun.*, 9 (2007) 1107.
17. E.M. Sorensen, S.J. Barry, H.K. Jung, J.R. Rondinelli, J.T. Vaughey, K.R. Poeppelmeier, *Chem. Mater.*, 18 (2006) 482.
18. A. Guerfi, S. Sevigny, M. Lagace, P. Hovington, K. Kinoshita, K. Zaghib, *J. Power Sources*, 119-121 (2003) 88.
19. D. Wang, N. Ding, X. Song, C. Chen, *J. Mater. Sci.*, 44 (2009) 198.
20. D. Bresser, E. Paillard, M. Copley, P. Bishop, M. Winter, S. Passerini, *J. Power Sources*, 219 (2012) 217.
21. Y.F. Tang, L. Yang, Z. Qiu, J.S. Huang, *Electrochem. Commun.*, 10 (2008) 1513.
22. F.O. Ernst, H.K. Kammler, A. Roessler, S.E. Pratsinis, W.J. Stark, J. Ufheil, P. Novák, *Mater. Chem. Phys.*, 101 (2007) 372.

23. H.Y. Koo, J.H. Yi, J.H. Kim, Y.N. Ko, Y.J. Hong, Y.C. Kang, B.K. Kim, *Powder Technol.*, 207 (2011) 362.
24. W.Y. Teoh, R. Amal, L. Madler, *Nanoscale*, 2 (2010) 1324.
25. G.L. Chiarello, I. Rossetti, L. Forni, *J. Catal.*, 236 (2005) 251.
26. T. Tani, L. Madler, S.E. Pratsinis, *J. Mater. Sci.*, 37 (2002) 4627.
27. J.H. Kim, H.Y. Koo, Y.N. Ko, J.H. Yi, Y.C. Kang, H.M. Lee, J.Y. Yun, *J. Ceram. Soc. Jpn.*, 117 (2009) 1311.
28. X. Zhang, H. Zheng, V. Battaglia, R.L. Axelbaum, *J. Power Sources*, 196 (2011) 3640.
29. X. Zhang, H. Zheng, V. Battaglia, R.L. Axelbaum, *Proc. Combust. Inst.*, 33 (2011) 1867.
30. T.W. Lee, K.H. Cho, J.W. Oh, D.W. Shin, *J. Power Sources*, 174 (2007) 394.
31. S.H. Choi, J.H. Kim, Y.N. Ko, Y.C. Kang, *Int. J. Electrochem. Sci.*, 8 (2013) 1146.
32. J.H. Kim, S.H. Choi, M.Y. Son, M.H. Kim, J.K. Lee, Y.C. Kang, *Ceram. Inter.*, 39 (2013) 331.
33. J.S. Cho, Y.C. Kang, *J. Alloys Compd.*, 464 (2008) 282.
34. C. Jiang, Y. Zhou, I. Honma, T. Kudo, H. Zhou, *J. Power Sources*, 166 (2007) 514.
35. K.S. Park, A. Benayad, D.J. Kang, S.G. Doo, *J. Am. Chem. Soc.*, 130 (2008) 14930.
36. Y.S. Hu, L. Kienle, Y.G. Guo, J. Maier, *Adv. Mater.*, 18 (2006) 1421.
37. D.W. Murphy, F.J. Di Salvo, J.N. Carides, J.V. Waszczak, *Mater. Res. Bull.*, 13 (1978) 1395.
38. C. Jiang, I. Honma, T. Kudo, H. Zhou, Electrochem. *Solid State Lett.*, 10 (2007) 127.
39. C. Jiang, M. Ichihara, I. Honma, H. Zhou, *Electrochim. Acta*, 52 (2007) 6470.